ANTICANCER RESEARCH *40*: 2613-2625 (2020)
doi:10.21873/anticanres.14232

3PO as a Selective Inhibitor of 6-Phosphofructo-2-Kinase/Fructose-2,6-Biphosphatase 3 in A375 Human Melanoma Cells

KRZYSZTOF KOTOWSKI[1], STANISŁAW SUPPLITT[2], DANIEL WICZEW[3], DAWID PRZYSTUPSKI[1], WERONIKA BARTOSIK[4], JOLANTA SACZKO[5], JOANNA ROSSOWSKA[6], MAŁGORZATA DRĄG-ZALESIŃSKA[7], OLGA MICHEL[5] and JULITA KULBACKA[5]

[1]*Faculty of Medicine, Wroclaw Medical University, Wroclaw, Poland;*
[2]*Department of Genetics, Wroclaw Medical University, Wroclaw, Poland;*
[3]*Faculty of Fundamental Problems in Technology, Wroclaw University of Science and Technology, Wroclaw, Poland;*
[4]*Faculty of Biotechnology, University of Wroclaw, Wroclaw, Poland;*
[5]*Department of Molecular and Cellular Biology, Wroclaw Medical University, Wroclaw, Poland;*
[6]*Hirszfeld Institute of Immunology and Experimental Therapy, Polish Academy of Sciences, Wroclaw, Poland;*
[7]*Department of Human Morphology and Embryology, Division of Histology and Embryology, Wroclaw Medical University, Wroclaw, Poland*

Abstract. *Background/Aim: The occurrence of $BRAF^{V600E}$ mutation causes an up-regulation of the B-raf kinase activity leading to the stabilization of hypoxia-inducible factor 1-alpha (HIF-1α) - the promoter of the 6-phosphofructo-2-kinase/fructose-2,6-biphosphatase 3 (PFKFB3) enzyme. The aim of the study was to examine the effect of the (2E)-3-(3-Pyridinyl)-1-(4-pyridinyl)-2-propen-1-one (3PO), as an inhibitor of PFKFB3, on human melanoma cells (A375) with endogenous $BRAF^{V600E}$ mutation. Materials and Methods: A375 cells were exposed to different concentrations of 3PO and the following tests were performed: docking, cytotoxicity assay, immunocytochemistry staining glucose uptake, clonogenic assay, holotomography imaging, and flow cytometry. Results: Our studies revealed that 3PO presents a dose-dependent and time-independent cytotoxic effect and promotes apoptosis of A375 cells. Furthermore, the obtained data indicate that 3PO induces cell cycle arrest in G1/0 and glucose uptake reduction. Conclusion: Taking all together, our research demonstrated a here should be proapoptotic and antiproliferative effect of 3PO on A375 human melanoma cells.*

Correspondence to: Julita Kulbacka, Department of Molecular and Cellular Biology, Wroclaw Medical University, Borowska 211A, 50-556 Wroclaw, Poland. Tel: +48 717840692, Fax +48 717840200, e-mail: julita.kulbacka@umed.wroc.pl

Key Words: Melanoma, $BRAF^{V600E}$, 3PO, A375, inhibitor, PFKFB3.

Malignant melanoma is a neoplasm derived from melanocytes (pigment-containing cells) localized typically in the skin as well as in the eye, intestines, inner ear and meninges (1). Its cutaneous form is considered as the most aggressive and the deadliest type of skin cancer. The primary locus of tumor exhibits a predilection for early metastasis, which can occur even from thin carcinomas. Therefore, the early diagnosis of melanoma is essential for the further success of the applied treatment (1).

Depending on the tumor's features, possible therapeutic methods may include surgery, chemotherapy, radiotherapy, immunotherapy or molecularly targeted therapies (2). Surgical excision of melanoma at the earliest possible stage is essential for a successful therapeutic outcome. Radiotherapy may be recommended for the treatment of skin, bone and brain metastases (3). Chemotherapy with dacarbazine, and temozolomide was the first systemic treatment applied in advanced melanoma; however, overall survival rates (OS) did not show significant improvement (4). In a phase III study comparing dacarbazine and temozolomide the response rate was 12% and 13%, respectively (5). None of these two alkylating agents affect a specific molecular pathway, thus they cannot be used in personalized oncology. Despite novel reports on new therapy achievements in the field of immunotherapy or biological treatment, these methods are insufficient and burdened with certain disadvantages and side-effects (6). This causes an urgent need for finding new treatment options for melanoma.

BRAF (v-raf murine sarcoma viral oncogene homolog B) gene is located at chromosome 7 (7q34) and encodes B-raf

kinase and its composed of 18 exones. BRAF mutation is localized mainly at codon 600 in exon 15 (7, 8). It occurs due to the transversion of thymidine (T) to adenosine (A) at nucleotide 1799 (T1799A), which causes substitution of valine (V) to glutamic acid (E), leading to what is called the $BRAF^{V600E}$ mutation. This mutation leads to the constant activity of B-raf kinase in the RAS-RAF-MEK-ERK pathway and is responsible for the aggressive character of BRAF mutant neoplastic cells (9).

Modern medicine strives to create targeted treatment precisely adjusted to the molecular profile of cancer, to enable the efficiency while limiting side effects from therapy. Targeted therapies of melanoma are based mainly on the BRAF mutation, which is observed in 50% of cases (10). Some drugs, such as vemurafenib and dabrafenib, inhibit the overactivated B-raf kinase (11). The effectiveness of these drugs has been proven, however, unfortunately, at the same time, alarming reports about their serious side effects (12) and the occurrence of acquired resistance (13) have been revealed.

An interesting alternative to the above-mentioned medicines might be selective inhibitors of the isoform 3 of 6-phosphofructo-2-kinase/fructose-2,6-bisphosphatase (PFK2/FBPase), the protein product of the *PFKFB3* gene. In the presence of $BRAF^{V600E}$ mutation, overactivated B-raf kinase enhances glycolysis *via* the activation of PFK2/FBPase (14). Kumar *et al*. (2007) have discovered that $BRAF^{V600E}$ mutation increases HIF-1α (hypoxia-inducible factor 1-alpha) expression (15). PFKFB3 promoter contains HIF-1α binding sites necessary for transactivation of this gene (16). Thus, HIF-1α factor, which is overexpressed in the case of $BRAF^{V600E}$ mutation, induces PFKFB3 expression. The product of reaction catalyzed by PFKFB3 – Fructose-2,6-diphosphate (F2,6BP) stimulates allosterically the activity of enzyme PFK-1 (17). The described mechanism leads to the phenomena included in what is called the Warburg's effect – the state of intensified glycolytic activity in tumor cells and their aggressive metabolism (Figure 1) (18, 19). The inhibition of such network of correlations may contribute to the changes in metabolism of tumor cells, giving a new insight into cytotoxic effects of PFKFB3-related factors.

PFK2/FBPase is present in the cytoplasm of human cells in the four isoforms. PFKFB3 (isoform 3) and PFKFB4 (isoform 4) are overexpressed in several cancer types, with PFKFB3 being the dominant one (21). Trojan *et al*. (2018) have described the presence of the PFKFB3 and PFBFB4 in the melanoma cells (22), suggesting that this enzyme may be an interesting target for melanoma treatment. Substances belonging to the PFKFB3 inhibitor group are able to inhibit this isoform (23), promoting stress in cancer cells. In the latter is expressed in the form of increased sensitivity to cytostatic agents or leading to apoptosis (24). The best-known representative of the PFKFB3 inhibitor group is (2E)-3-(3-Pyridinyl)-1-(4-pyridinyl)-2-propen-1-one (3PO; Figure 1B). 3PO has been shown as a cytotoxic agent for hepatocellular carcinoma (19), Jurkat T Cell Leukemia Cells (25), human colon and bladder cells (26). Moreover, 3PO does not affect the level of glucose in erythrocytes and white blood cells during daily *in vivo* administration. This is particularly important since glycolysis is the only glucose metabolism pathway in the red blood cells in mammals (16). Taking altogether the aforementioned findings, we hypothesized that 3PO may inhibit the proliferation of melanoma cells and display a cytotoxic effect on them.

In our study we aimed to evaluate an effect of PFKFB3 blockade on A375 human melanoma cells with the use of 3PO. We hypothesized that inhibition of PFKFB3 contributes to the decrease of $BRAF^{V600E}$-positive melanoma cells' viability.

For the purpose of this research, the A375 melanoma cell line was chosen. According to literature, the hyperactivation of ERK pathway by the $BRAF^{V600E}$ mutation is the main factor of tumorigenesis in A375 cells (27, 28). For this reason, we picked the A375 melanoma cell line as a proper model to investigate the consequences of inhibition of BRAF-related molecular phenomena.

Materials and Methods

Docking and computational analysis. The model of the ligand was prepared using the Avogadro Software 1.2.0 (Avogadro Chemistry, an open-source molecular builder and visualization tool. Version 1.2.0. http://avogadro.cc/) (29), and then the ligand's geometry was initially optimized using the MMFF94 (30) force field. In the next step, to ensure the proper geometry, *ab initio* calculations were conducted using the Gaussian 16 B.01 software (Gaussian inc., Wallingford, CT, USA) (31), double hybrid B2PLYPD3 (32) density functional with Grimme D3J dispersion correction and Def2SVP (33) double zeta basis set. After the optimization, the ligand was saved as a PDBQT file with a torsional tree generated for docking calculations.

Concerning the protein, the crystallographic structure of Human PFKFB3 in complex with an indole inhibitor with resolution 2.5 Å (23) was taken from the Protein Data Bank (PDB CODE: 5AJW) and was saved as a PDB file. Furthermore, water molecules, inhibitors, and phosphates were removed from the crystallographic structure. After that, the protein was saved in PDBQT format without the generation of the torsional tree, because the protein will be kept rigid during docking.

The previously prepared PFKFB3 protein model was docked with a prepared ligand model using Smina 1.0.0 (open-source software) (34), and Autodock Vina (35) modification. Furthermore, the Vinardo (36) scoring function (called Smina/Vinardo) was chosen for a more accurate representation of energy interactions between protein and ligand, and the search space was spanned over the whole protein due to limited information about the docking site. The Vinardo scoring function correlates with experimental data similarly to the X-Score scoring function that is significantly better than the LIDO used in the previous docking study, ensuring that the modelling results are closer

to the reality (19, 37). The docking procedure was repeated 50 times, and 20 poses for each repeat were generated. The pose with the lowest energy among all repeats was chosen for further visualization and analysis and was visualized using the Visual Molecular Dynamics (VMD) software 1.9.2 (Beckman Institute, Urbana, IL, USA) (38).

Also, an additional docking protocol was performed using AutoDock 4 (Olson Laboratory, La Jolla, CA, USA) to confirm the results obtained with Smina/Vinardo. To do this the AutoDock 4.2.6 was used together with AutoDockTools software (33). The system was prepared the same way as Smina/Vinardo, the search space was spanned over the whole protein. As Autodock 4 requires partial charges, these were obtained from the Gasteiger Partial Charges in the AutoDockTools for protein as for the 3PO ligand. After that, the grid map was generated based on the search space defined previously. Further, the docking settings were chosen, the Lamarckian Genetic Algorithm was used to explore the conformational and search space. The number of energy evaluations was set to 2.5×10^7 and the rest was left as default. The pose with the lowest energy among all repeats was chosen for further visualization and analysis using the Visual Molecular Dynamics (VMD) software.

Cell culture. The melanoma A375 cells that express endogenous $BRAF^{V600E}$ mutation - (ATCC® CRL 1619™ , London, UK) were used for our experiments. Cells were cultured as a monolayer on polystyrene cell culture flasks (Falcon®, Corning Life Sciences, Tewksbury, MA, USA) with DMEM (Dulbecco's Modified Eagle's medium, Sigma-Aldrich, Saint Louis, MO, USA) containing 10% fetal bovine serum (FBS, Sigma-Aldrich), 20 U/ml penicillin and streptomycin 20 µg/ml (Sigma-Aldrich). Cells were incubated at 37˚C with 5 % CO_2 in a humified incubator (Heraeus®, Thermo Fisher Scientific, Waltham, MA, USA). Prior to the experiment, cells were detached using Trypsin 0.25% and EDTA 0.02% (Sigma-Aldrich).

Drugs. (2E)-3-(3-Pyridinyl)-1-(4-pyridinyl)-2-propen-1-one were produced by Sigma-Aldrich (Sigma, cat. no. SML1343). Each drug solution was freshly prepared directly before the experiment. First, 3PO was dissolved in DMSO (Sigma-Aldrich, cat. no. 41639) to a 5 mM concentration (stock solution) and was subsequently diluted to a 5-200 µM concentration in cell culture medium (DMEM) for further tests.

MTT assay. The MTT assay is based on a colorimetric method, allowing for indirect evaluation of the cell viability. In this assay, the cell survival was reflected in the activity of mitochondrial dehydrogenases which metabolize the yellow, water-soluble tetrazolium salt (MTT) to the purple, water-insoluble formazan crystals.

At first, A375 cells were seeded in 96-well plates at the concentration of 50 000 cells/well in 150 µl of growth medium and subsequently, 24 h after culturing, cells were incubated in medium alone (control) or in medium containing various concentrations of 3PO: i) 5 µM, ii) 10 µM, iii) 15 µM, iv) 25 µM, v) 50 µM, vi) 75 µM, vii) 100 µM and viii) 200 µM. After 24 or 48 h, growth medium was removed and replaced by the MTT solution (0.5 mg/ml PBS buffer). Next, the cells were cultured with MTT at 37˚C for 3 h. After that, the formed formazan crystals were dissolved in acidified isopropanol (100 µl/well, 0.04 M HCl in absolute isopropanol per well). The absorbance was measured using the multiplate reader at 570 nm (EnSpire Multimode Plate Reader, Perkin Elmer, Waltham, MA, USA). The viability of the non-treated control cells was considered as the 100% of survival.

Immunocytochemical staining. Immunocytochemistry was performed 24 h after treatment on cells. At first, cells were fixed in 4% paraformaldehyde (Roth, Germany). Then, immunocytochemical detection using horseradish peroxidase (HRP) was performed. The following antibodies were used: rabbit polyclonal caspase-3 antibody (cat. no. LF-MA0030, Thermo Fisher Scientific Inc., distr. Life Technologies, Warsaw, Poland) and mouse monoclonal antibody against caspase 8 (Santa Cruz Biotechnology Inc., Dallas, TX, USA, cat. no. sc-56070). Caspase-3 and -8 antibodies were diluted in an IHC Select® Antibody Diluent Solution (Sigma-Aldrich, cat. no. 21544) at a dilution of 1:200. After overnight incubation, the antigens were visualized using the EXPOSE Mouse and Rabbit Specific HRP/DAB Detection IHC kit (Abcam, Cambridge, MA, USA, cat. no ab80a36) following our protocol from an earlier study (39). Finally, cells were stained with hematoxylin for three min to visualize nuclei, dehydrated in an increasing concentration of EtOH, cleared in xylene and mounted in DPX (Sigma Aldrich, cat. no. 100579). Then, the microscopic sides were examined with the upright microscope (Olympus BX51, Tokyo, Japan). The percentage of stained cells was estimated manually by two independent researchers and the intensity of immunocytochemical reaction was evaluated according to the scale: (–) negative, (+) weak, (++) moderate and (+++) strong.

Cell death analysis. A375 cells were plated at a concentration of 120 000 cells/well in a 6-well dish in 2.0 ml complete medium and 48 h after seeding, they were incubated for 24 h in medium alone or in medium with the following concentrations of 3PO: i) 5 µM, ii) 25 µM, and iii) 100 µM. After that, the cells were washed and detached. The collected growth medium and cell suspension were centrifuged (6,720 × *g*) for 10 min at 4˚C. Next the cells were stained with Annexin-V labeled with FITC and propidium iodide (PI) (Annexin V-FITC Apoptosis Detection Kit, BioVision Inc, Milpitas, CA, USA cat. No. K101-100) following the protocol described by Crowley *et al*. (40). For the excitation blue laser 488 nm was used and for detection green detector for FITC, and red I detector for PI respectively. Finally, cells were analyzed using flow cytometry (CUBE6, Sysmex, Poland).

Clonogenic assay. A clonogenic assay was performed after a 24-hour incubation in 5, 25 and 100 µM concentration of 3PO, and then 1×10^3 cells per well were seeded in 6-well plates in DMEM (Dulbecco's Modified Eagle's medium). After 7 days of incubation, the colonies were fixed following the Franken's Nature Protocols (41). Formed colonies were counted using ImageJ 1.52q software (National Institute of Health, Bethesda, MD, USA).

Glucose uptake analysis. Glucose transport inside the cell was measured by the bioluminescence of the 2-deoxyglucose-6-phosphate that accumulates in cells uptaking glucose derivatives in this assay. The cells were plated in 96-well plates at a concentration 5×10^4 per well and 24 h after seeding, the cells were incubated for additional 24 h in different concentrations of 3PO (5, 25 and 100 µM). Next, the cells were washed, detached, and 50 µl of 1 mM 2DG were added to every well for a 10-minute incubation. Then, we added 25 µl of Stop Buffer (Glucose-Glo™ Assay, Promega Corporation, Madison, WI, USA, cat. No. J6021) and an equal volume (25 µl) of

Neutralization Buffer (Glucose-Glo™ Assay, Promega Corporation, cat. no. J6021). Subsequently, we incubated with 100μl of G6PHD Detection Reagent for 1 hour. The bioluminescence was measured using the Promega GloMax® Discover System multiplate reader (Promega Corporation) choosing "Glucose Uptake-Glo™ protocol".

Cell cycle profiling. Cells were cultured in a 6-well plate at a concentration of 5×10^5 per well and were incubated with 3PO at the following concentration: 5, 25 and 100 μM. Next, the cells were harvested and fixed in cold ethanol (70 %) at 4 ˚C for 12 h, washed and resuspended in phosphate-buffered saline (PBS), incubated with 100 μg/ml RNAse (A&A Biotechnology, cat. no. 1006-10), and stained with 50 μg/ml propidium iodide (PI; Sigma Aldrich, cat. no. 81845) solution in the dark for 30 min. A content was assessed by the Becton Dickinson FortessaÔ Cell Analyzer (Franklin Lakes, NJ, USA) using the FACSDiva software.

Statistical analysis. All experiments were performed in triplicate for each parameter, which gives 9 repetitions for each parameter. Data are expressed as mean±standard error of the mean. Data were analyzed by two-way ANOVA (in GraphPad Software Inc., San Diego, CA, USA), with p-Value<0.05 being considered statistically significant. IC_{50} values were calculated by nonlinear regression (curve fit) of cytotoxicity data using a sigmoidal dose-response (variable slope) equation.

Results

3PO binds to active site of PFKFB3. The 3PO has been identified as a PFKFB3 ligand based on the molecular docking using LIDO and a homology model of PFKFB3 using the PFKFB4 structure (14). Nevertheless, the affinity of the ligand has not been revealed, while it has also not been compared to its native ligand F-2,6-BP (21).

Since there is no binding affinity data for the 3PO ligand, the identification of the binding site for 3PO by B. Clem *et al*. in 2008 (19) is rather suspicious, due to the use of a rather inaccurate LIDO scoring function and homology modelling.

We have decided to perform a molecular docking simulation using the crystallographic structure of PFKFB3. The docking results revealed that 3PO binds to the F-2,6-BP binding site of PFKFB3 and shares amino acids with the fructose-6-phosphate. The binding site of crystallographic F-2,6-BP and docked 3PO are shown in Figure 2A. There are 7 amino acids within 3Å which bind to the 3PO and also the F-2,6-BP (see Figure 2C). It shows that 3PO binds to 2-Pase domain similar to the native ligand F-2,6-BP. Consequently, the 3PO blocks the release of the phosphorylation product (F-2,6-BP) from the 2-Pase domain. Furthermore, in comparison to the native ligand – F-2,6-BP, the 3PO seems to interact with 3 additional amino acid residues, consequently, it binds more strongly and has higher affinity than the native ligand (Figure 2C).

According to the results of the previous docking study by B. Clem *et al*. in 2008, the identified binding site for 3PO was the 2-Kase domain, which binds Fructoso-6-Phosphoran (19). Due to the contradictory results between our and their study, we decided to perform a docking simulation using another docking software – Autodock 4. Our results (Figure 2A) are the same as with the Smina/Vinardo; 3PO binds to the 2-Pase domain; however, these need to be confirmed experimentally.

Furthermore, the binding free energy $\Delta G_{binding}$ of the best 3PO pose obtained from the docking calculations using Smina/Vinardo was –7.5 kcal/mol, while –7.78 kcal/mol was obtained for Autodock 4. To interpret the results further in the study, the dissociation constant (*Kd*) was calculated for the temperature of 37˚C. The *Kd* is defined in relation to the binding free energy as:

$$\Delta G_{binding} = RTln\left(\frac{K_d}{1M}\right)$$

where R is the ideal gas constant

$$\left(1.985\frac{cal}{mol\cdot K}\right)$$

T is the temperature of the studied system, *Kd* is the dissociation constant and [1*M*] is reference concentration of 1*M*/*l*. By rearranging the equation, *Kd* can be calculated as shown below:

$$K_d = e^{\frac{\Delta G_{binding}\cdot c^{\Theta}}{RT}}$$

By substituting the temperature and the binding energy in *cal/mol* the resulting dissociation constant *Kd* has a value of 5.2×10^{-6}, which translates to 50% of PFKFB inhibition in a concentration of 5.2 μM. The molecular docking calculation reveals the optimum concentration of 3PO that needs to be administered to promote the desired effect. In this case, this concentration is high.

The reason behind choosing the binding free energy from the Smina/Vinardo is that it has better accuracy compared to Autodock Vina alone, which in turn has a better accuracy compared to Autodock 4 (35, 36). Nevertheless, the results are close in both cases.

Cytotoxic effect of 3PO on A375 melanoma cells. The MTT assays revealed that 3PO showed a cytotoxic effect on A375 melanoma $BRAF^{V600E}$ -positive cells in a dose-dependent manner (Figure 3). We observed a significant decrease in cell survival after 24 h of incubation with 3PO at a concentration higher than 50 μM. Similar findings were noted when the cells were cultured for 48 h with 3PO at a concentration higher than 75 μM (Figure 3A). Cell viability estimated by mitochondrial activity as measured by the MTT assay at concentrations above 25 μM revealed an exponential

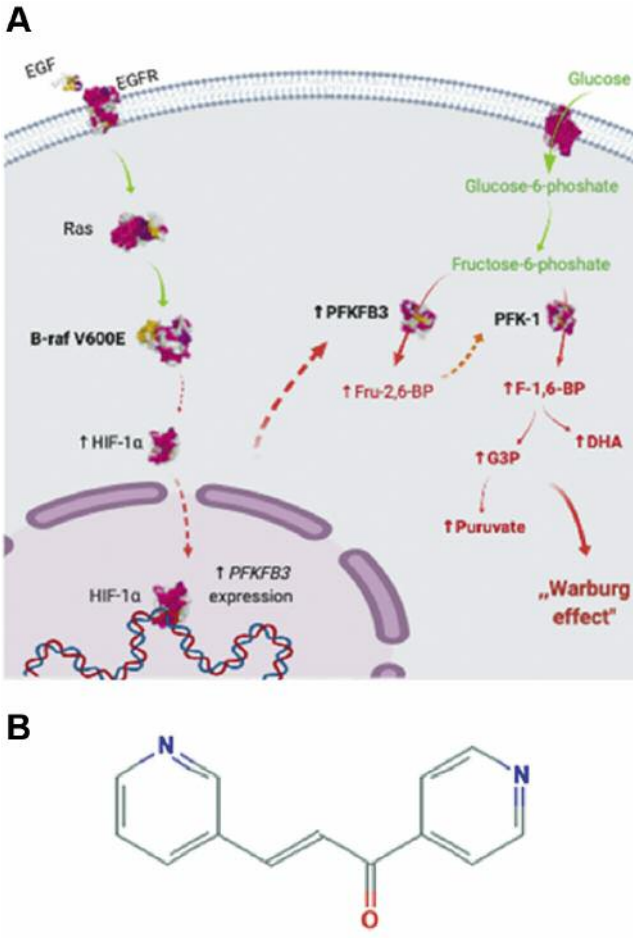

Figure 1. *The schematic presentation of the molecular basis of targeting PFKFB3 as a therapeutic strategy against melanoma (A) (Adapted from Ref. 19) and (B) the 2D structure of 3PO (20). EGR: Epidermal growth factor; EGFR: epidermal growth factor receptor; HIF-1α: hypoxia-inducible factor α; Fru-2,6-BP: fructose 2,6-bisphosphate; F-1,6-BP: fructose 1,6-bisphosphate; PFK-1: phosphofructokinase-1; PFKFB3: 6-phosphofructo-2-kinase/fructose-2,6-bisphosphatase isoform 3; DHA: dihydroxyacetone: G3P: glyceraldehyde 3-phosphate.*

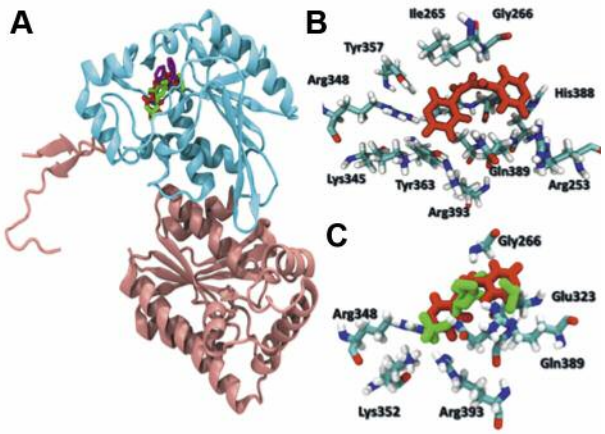

Figure 2. *Simulation of the 3PO binding efficacy: A) docking of the 3PO ligand using the Smina/Vinardo (red) and docking of the native ligand F-2,6-BP using the Autodock 4 (green). The 3PO binds to the 2-Pase domain, same as the F-2,6-BP native ligand, indicating why it inhibits the PFKFB3. The 2-Pase domain is shown in the cyan color, where the 2-Kase domain is shown in brick color. B) Amino acids within 3Å of the 3PO docked ligand. The number near the amino acid's name indicates a position in the protein structure. The two amino acids at the back of the image are glutamine 322 and isoleucine 323. C) Amino acids, that are shared between the docked 3PO ligand and the docked F-2,6-BP native ligand. The amino acids are shown within 3Å of both ligands.*

downward trend which corresponds to the logarithmic increase of the PFKFB3 inhibition. The lowest mitochondrial activity was observed after 48 h of incubation at a concentration of 200 μM 3PO. Between 24 and 48 h of incubation, no significant difference between any 3PO concentrations was obtained. The calculated IC_{50} for 24 and 48h of incubation with 3PO were 114.0 and 104.1 μM, respectively.

Microscopy observations showed dose-dependent changes in cell morphology, with effects becoming noticeable when the cells were cultured with 25 μM of 3PO (Figure 3B). These effects include cell regression and increased number of protrusions. The cells exposed to 3PO for 48 h presented more of the described changes. Holotomographic microscopy showed a reduction in the size of cells exposed for 24 h at increasing concentrations of 3PO (Figure 3C).

Apoptosis prevails over necrosis in 3PO-treated A375 melanoma cells. Cell death evaluated with flow cytometry (Figure 4) revealed an increased percentage of all damaged cells at the concentration of 100 μM 3PO compared to control (8.93% *versus* 25.05%). Our study revealed that apoptosis, recognized by Annexin V staining (a marker of phosphatidylserine representation on the cell surface) prevails over necrosis (indicated as the propidium iodide influx through disturbed cell membranes) in cells incubated with the analyzed concentrations of 3PO. In fact, the predominant process of cell death in our experiments with 3PO was early apoptosis. Our research revealed that 24.38% of all apoptotic cells among the population of cells incubated with 100 μM 3PO were going through early apoptosis, as revealed by the fact that cells were bound to annexin V but excluded PI (42) (Figure 4) (Table I).

3PO induces caspase - related apoptosis. The performed immunocytochemical reaction revealed 3PO dose-dependent caspase 3 (executive caspase) and caspase 8 (initiator caspase) expression in A375 cells. A significant difference in both caspase-3 and caspase-8 was observed already at the lowest given concentration of the 3PO (25 μM) (Figure 5).

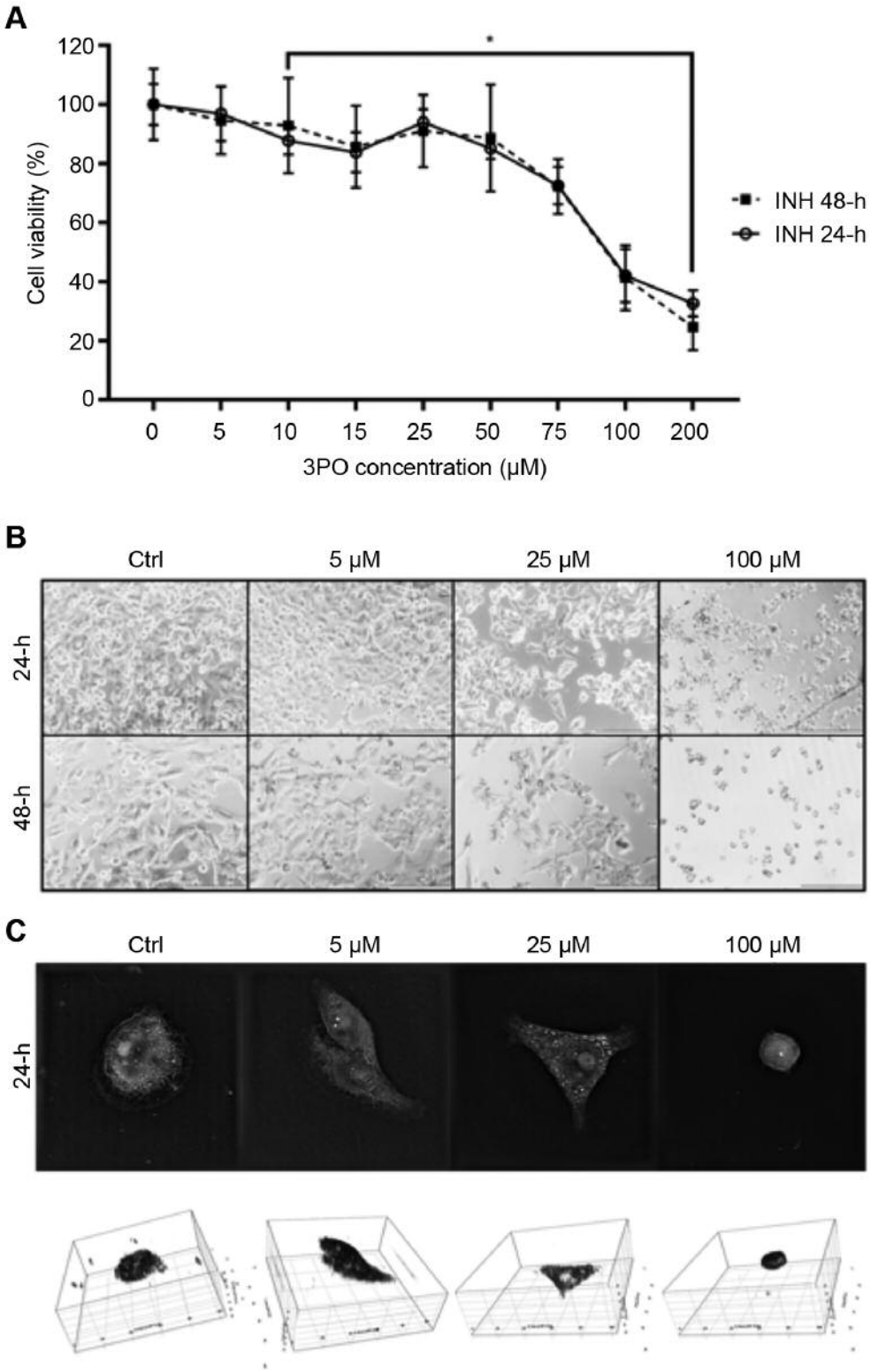

Figure 3. *Cytotoxic effect of 3PO on A375 melanoma cells: A) Viability of A375 cells after 24 and 48 h of incubation with 3PO measured using the MTT assay. B) Morphology of the A375 melanoma cells incubated in medium without (Ctrl) or with 3PO at a concentration of 5, 25 and 100 μM. C) Morphology of the A375 melanoma cell line incubated in medium alone (Ctrl) or medium with 3PO at a concentration of 5, 25 and 100 μM. The pictures and 3D representations were acquired using the holotomography microscope (3D Cell Explorer, Nanolive). *p<0.05. Scale bars: 200 μm. INH: Inhibition.*

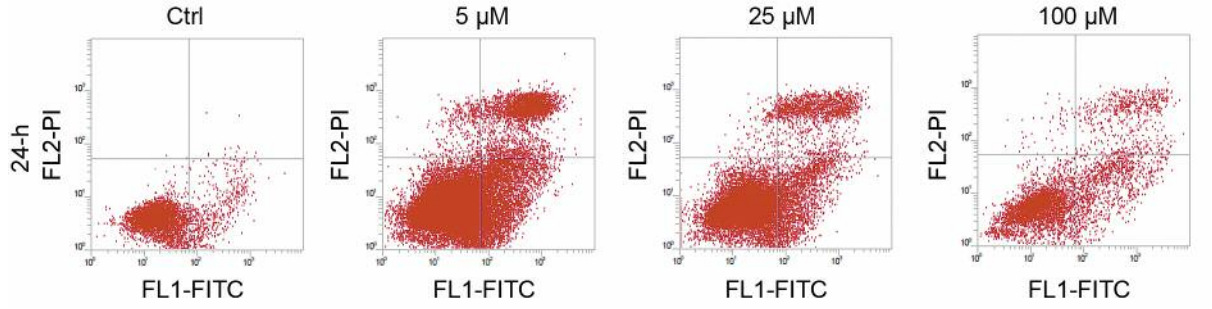

Figure 4. *Cell death evaluation of A375 cells after 24 h of incubation without 3PO (Ctrl) and with 3PO at the concentration of 5, 25 and 100 μM (staining with Annexin-FITC and PI).*

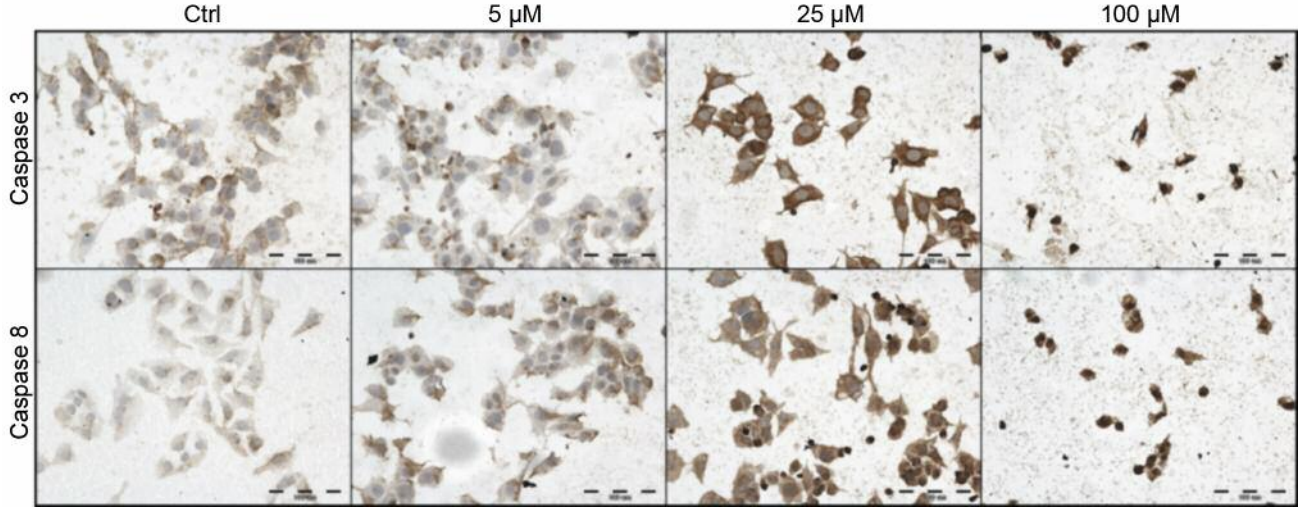

Figure 5. *Apoptosis intensity after 24h incubation with 3PO. The representative microscopy images present cytoplasmatic expression of caspase 3 and 8 in A375 melanoma cells. The IHC reaction is stronger in cells exposed to the higher 3PO concentrations. Scale bars: 100 μM.*

Table I. *Cell death evaluation of A375 cells after 24 h of incubation with 3PO. Results are expressed as percentage of cells.*

Concentration	Unstained	Necrotic	Early apoptotic	Late apoptotic
Ctrl	91.07%	0.03%	8.64%	0.26%
5 μM	86.20%	0.41%	8.37%	5.01%
25 μM	84.61%	0.51%	9.32%	5.56%
100 μM	74.95%	0.67%	15.39%	8.99%

Table II. *The immunocytochemical reaction with caspases 3 and 8 antibody in A375 cells after 24 h of incubation with 3PO.*

	Caspase 3		Caspase 8	
Concentration	% of stained cells	Reaction intensity	% of stained cells	Reaction intensity
Ctrl	98%	–/+	97%	–/+
5 μM	96%	+/++	100%	++
25 μM	100%	+++	98%	+++
100 μM	100%	+++	100%	+++

The most intense staining of the two antibodies was observed at the highest concentration of 100 μM we tested (Table II).

3PO inhibits glucose uptake. Glucose metabolism was also affected in A375 cells cultured with 3PO. The collected data reported the influence of PFKFB3 inhibition on the glucose uptake of these cells (Figure 6). At the lowest investigated 3PO concentration (5 and 25 μM) glucose uptake was increased; however, at the highest concentration (100 μM) there was a significant reduction of glucose uptake (Table III).

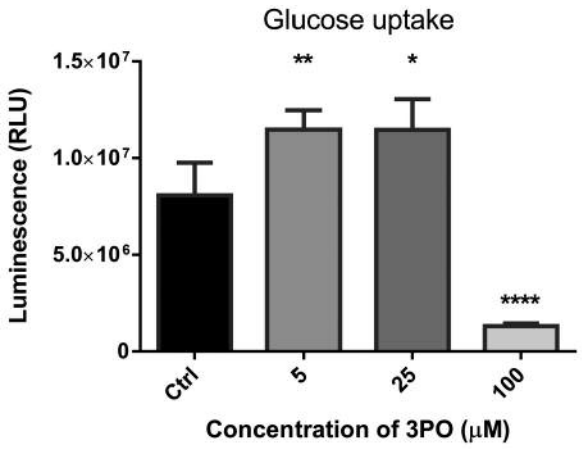

Figure 6. *The glucose uptake in A375 cell line after 24 h of incubation with 3PO. *p<0.05, **p<0.01, ****p<0.0001 compared to control. RLU: Relative luminescence units.*

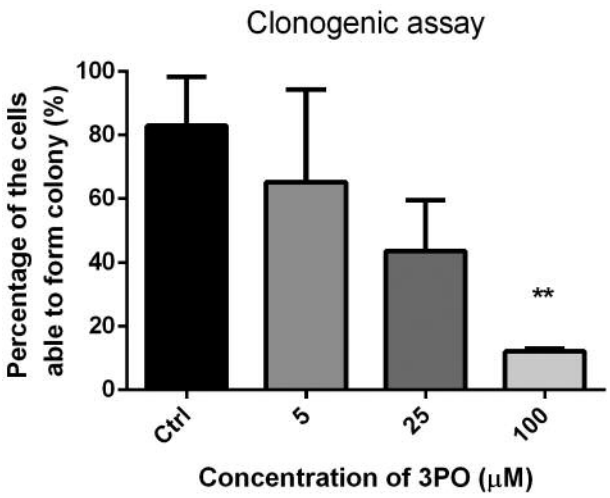

Figure 7. *Clone formation efficacy in A375 cell line after 24 h of incubation with 3PO. **p<0.01 compared to control.*

Table III. *The glucose uptake in A375 cell line after 24 h of incubation with 3PO. RLU: Relative luminescence units.*

	Ctrl	5 μM	25 μM	100 μM
Luminescence (average) (RLU)	9.23e+06	1.15e+07	1.03e+07	1.31e+06

Table IV. *The clonogenic assay in the A375 cell line after 24 h of incubation with 3PO. The results are represented by the percentage of cells able to form colonies.*

	Ctrl	5 μM	25 μM	100 μM
Percentage of seeded cells able to form colonies (%)	82.96%	65.22%	43.52%	12.12%

3PO influence on proliferation process. Using the clonogenic assay we revealed that a 24 h incubation with different concentrations of 3PO inhibited the cell division process (Figure 7). The percentage of colonies arising from seeded cells decreased in an inversely proportional manner to the 3PO concentration, with up to 60.72% colony formation decrease at the highest investigated 3PO concentration (100 μM) (Table IV).

3PO induces cell cycle arrest in A375 melanoma cells. To determine whether 3PO affects cell cycle we performed FACS analysis of the cells treated with 3PO for 24 h. Our studies revealed that 24 h incubation with 3PO increased the percentage of cells in the G1/0 phase and simultaneously decreased the percentage of cells in the S phase. Among the cells incubated without the 3PO, the G1/0 phase was the cell cycle phase with the longest duration and was observed in 45.3% of examined A375 cells. Low 3PO concentrations of 5 and 25 μM did not cause significant changes in the percentage of cells in G1/0 or S phase. However, when cells were treated with 100 μM of 3PO there was an increase of up to 64.6% of cells in G1/0 and a decrease of the percentage of cells in S phase up to 12.4% (Figure 8).

Discussion

Nowadays 132,000 melanoma cases occur globally each year (43, 44). Melanoma is characterized by aggressive growth and unsatisfactory response to standard cytostatic treatment. BRAF mutation is a common mutation in melanomas, with about 90% $BRAF^{V600E}$ mutations (10). Unfortunately, the effectiveness of available BRAF inhibitors, such as vemurafenib, cause serious side effects, including cutaneous squamous cell carcinoma, cutaneous side effects, (*e.g.* pruritus, actinic keratosis, and photosensitivity) (45) and cardiotoxicity (12). Moreover, there are numerous reports concerning the occurrence of acquired resistance to these inhibitors (46). Taken together, these facts signify the importance of identifying new treatment options for melanoma.

Based on the fact that a great number of cancer cells present an increased level of the PFK2/FBPase enzyme (25), inhibitors of this enzyme could be an interesting alternative for anti-neoplastic treatment. In fact, the cytotoxic effect of PFKFB3 inhibition has been previously revealed in the following cell lines: K562 (chronic myelogenous leukemia), HL-60 (acute promyelocytic leukemia) and MDA-MB231 (metastatic breast cancer adenocarcinoma) (19). In our

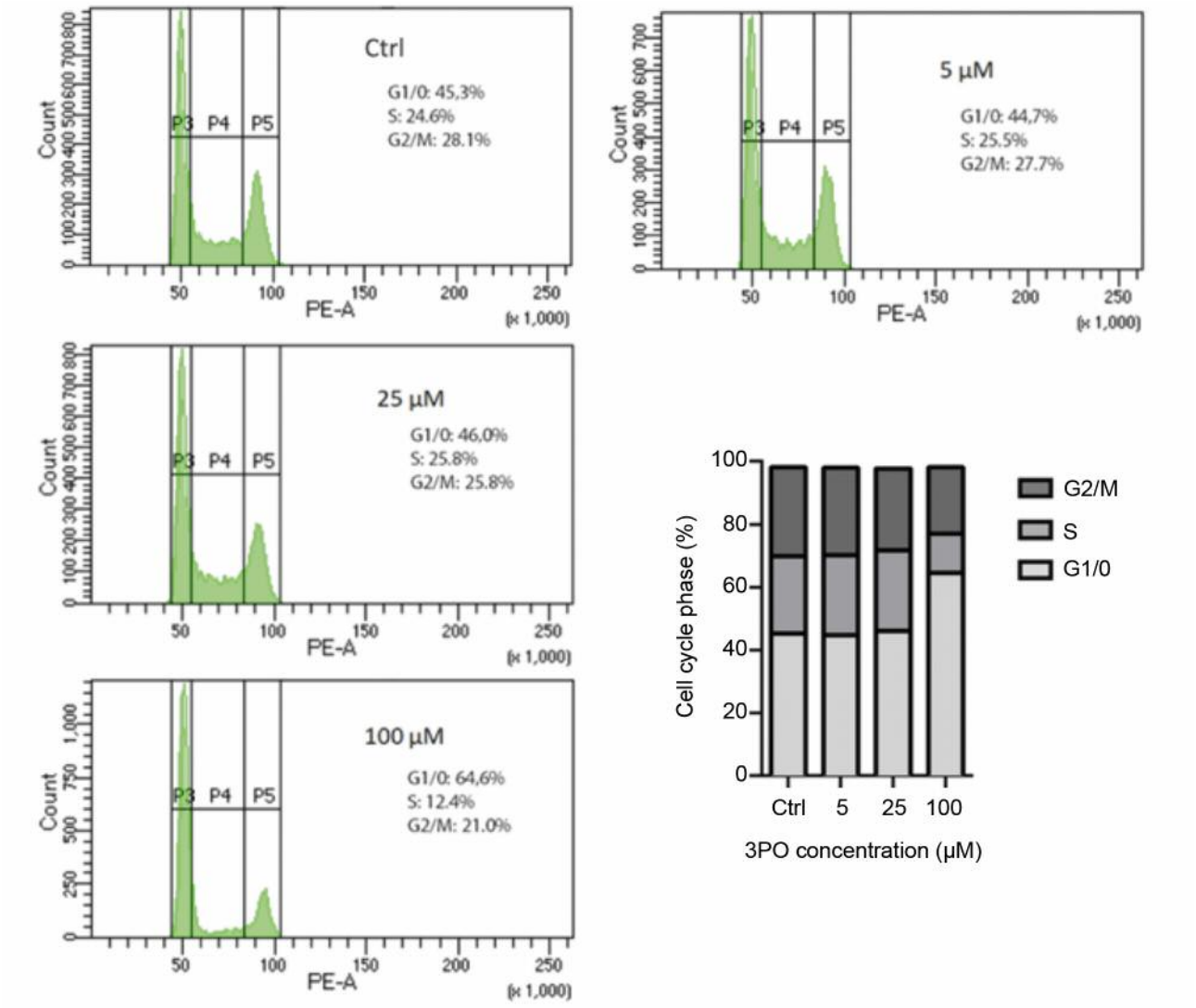

Figure 8. *Cell cycle analysis of A375 cells presented as histograms of PI intensity staining after 24 h of incubation with different 3PO concentrations and its summary (bottom right graph).*

studies we observed partially similar findings, with a dose-dependent 3PO-induced anticancer effect on A375 melanoma cells.

Xintaropoulou *et al*. (2015) studies have revealed that the cytotoxic effect of 3PO is associated more with apoptosis rather than with necrosis (47). Our studies confirmed that in A375 melanoma cells necrosis does not play a significant role in cell death induced by 3PO, as apoptosis was the dominating cell death process in all the tested 3PO concentrations. The induction of apoptosis was through the activation of a caspase-dependent pathway following incubation with 3PO. Similar results have been observed by Chowdhury *et al*. (2017) who used PFKFB3-targeted shRNA in A549 and H460 cells causing an increase in caspase 3 expression (48). In many cancer cells, PFKFB3 plays an important role in cell survival, as it is a downstream substrate of the mTOR kinase signaling pathway (49). The mTOR kinase is one of the main enzymes involved in cell cycle. The overexpression of this kinase is observed in various types of cancer (50). The up-regulation of the PFKFB3 expression is caused by the activation of mTOR kinase by HIF, whereas knocking down PFKFB3 inhibits mTOR activation and promotes apoptosis (49).

Apart from apoptosis, PFKFB3 inhibition also affects another type of cell death, autophagy. Klarer *et al*. in 2014 proved that the increase in HCT-116 colon adenocarcinoma cells autophagy was linked to their exposure to 3PO, and that this process was associated with LC3-II and p62 proteins (51).

Furthermore, Wang *et al*. in 2018 revealed that inhibition of PFKFB3 using of PFK-15 inhibits autophagy in rhabdomyosarcoma cells. Moreover, the same group observed an up-regulation of the LC3-II and p62 after 2 h of incubation with PFK-15; however, 12 h later LC3 further increased whereas p62 decreased. Moreover, PFK15 incubation also decreased pAMPK levels, suggesting that autophagy was inhibited by PFK15, and thus, AMPK acted downstream of PFKFB3. Combination of chloroquine and PFKFB3 inhibitors decreased the levels of LC3-II and autophagosomes in rhabdomyosarcoma cells (52). Decreased LC3 levels were also observed by Yan *et al*. in 2017, who, however, observed increased levels of p62 after 2 h of PFKFB3 inhibition (53), collectively suggesting that p62 may be involved only in the autophagy induction and then it decreases with time. Importantly, this study also proved that PFKFB3 mediates autophagy through the AMPK pathway (53).

Inhibition of glucose metabolism can affect glucose uptake. Klarer *et al*. (2014) has shown that PFKFB3 siRNA suppresses glucose uptake in HCT-116 cells (51). In our study, we observed a reduced glucose uptake after incubation with 3PO; however, in the lowest investigated concentrations, we observed a slight increase of glucose uptake that could be related to competitive PFKFB3 inhibition by 3PO. The latter effect could be blocked by adding the fructose-6-phosphate, which uses an allosteric mechanism of PFK-1 regulation. Based on these we cannot exclude that the observed glucose reduction in the highest evaluated concentrations could be the result of the cytotoxic influence of 3PO on the melanoma cells that also observed in these concentrations.

The reduced number of colonies in the clonogenic assay demonstrates the inhibitory effect of 3PO on the proliferation of A375 cells in a dose-dependent manner. This correlates with the work by Hamanaka *et al*. (2017), who have shown that incubation with 3PO and 2-DG inhibits nHEK proliferation (54).

Among the PFKFB3 up-to-date studied inhibitors, the best known are (2E)-3-(3-Pyridinyl)-1-(4-pyridinyl)-2-propen-1-one shortly, named as 3PO, and 1-(4-Pyridinyl)-3-(2-quinolinyl)-2-propen-1-one, known as PFK15 (55). Apart from the proapoptotic effect, the PFKFB3 inhibitors may promote other changes in the cell metabolism, such as a decrease of mitochondrial activity or induction of the cell cycle arrest. Zhu *et al*. have revealed that PFK15 induces cell cycle arrest in G1/G0 phase in gastric cancer cells by blocking the Cyclin-CDKs/Rb/E2F signaling pathway (56). Yalcin *et al*. have confirmed that PFKFB3 promotes cell cycle progression and suppresses apoptosis *via* Cdk1-mediated phosphorylation of p27 (57). Finally, Clem *et al*. have revealed that 3PO induces the suppression of cell proliferation as a result of the G_2-M phase cell cycle arrest (19). In our studies, we observed the occurrence of cell cycle arrest in G1/0. These data suggest that there might be different mechanisms of cell cycle arrest induced by PFKFB3 inhibitors in different cell lines.

Through the detailed analysis of the obtained data, we claim that the PFKFB3 inhibitors might be considered as novel agents for future use in melanoma treatment. It is worth mentioning that due to the selective nature of 3PO it does not cause hemolysis (14). Moreover, 3PO enhances the cytotoxic effect of cisplatin not only in platinum-sensitive but also in platinum-resistant ovarian cancer cells (58). Additionally, PFKFB3 induces autophagy as a survival mechanism by suppressing glucose uptake (51). Last, another 3PO derivative, PFK158, acts as a potent PFKFB3 inhibitor that synergizes vemurafenib to promote proapoptotic properties in A375 melanoma cells (59).

Unfortunately, the concentration at which 3PO is effective against melanoma cells turns out to be relatively high. This concentration is difficult to achieve in the clinic because of the poor solubility of 3PO in water. This is further supported by our docking data, which shows that the concentration of 3PO required to inhibit PFKFB is of the micromolar order. This information is important, especially due to data collected by Conradi *et al*., who have revealed that a low dose of 3PO (25 mg/kg) induces tumor vessel normalization by vascular barrier tightening, which may cause suppression of extravasation and metastases. On the contrary, a high dose of 3PO (70 mg/kg) may result in tumor vessel disintegration, and, as a consequence, aggravate tumor hypoxia but, unfortunately, it also promotes tumor dissemination (60).

Despite the mentioned limitations, these may be solved by the use of some novel methods to increase the drug effectiveness, such as with the use of nanocarriers (61) or specific modifications in the chemical structure of the drug to increase its solubility (62). Effectiveness may be also increased by using methods such as electroporation (63) or sonoporation (64).

Besides these disadvantages, low cytotoxicity, the ability to inhibit the proliferative potential of cancer cells, the influence on angiogenesis and the specificity of the 3PO suggest that it may become an important agent used in the medical treatment against melanoma in combination with other cytostatic drugs or BRAF kinase inhibitors.

In conclusion, this study demonstrated the influence of 3PO as a small molecule competitive inhibitor of PFKFB3 on A375 melanoma cells with endogenous $BRAF^{V600E}$ mutation. The presented results reveal the proapoptotic and antiproliferative, dose-dependent effect of 3PO in these cells. The disadvantage of this agent in clinical use for melanoma treatment might be its weak water solubility and especially inadequate binding affinity to the active site of PFKFB3. However, based on our findings, we suggest that an improved derivative of 3PO or other inhibitors of PFKFB3 may become innovative synergistic agents to be used in melanoma treatment in the following years.

Conflicts of Interest

The Authors declare no conflicts of interest.

Authors' Contributions

K.K contributed towards conceptualization, data analysis, and writing the results, discussion and conclusions. S.S. contributed to writing the introduction, to data curation, review and editing. D.W. contributed to writing the docking methodology and results. W.B. contributed to writing the methodology, and for review and editing. D.P, J.R and M.D.Z contributed to data curation and validation. J.K. contributed to conceptualization, data analysis, supervision and final review and edition. J.S. and O.M. contributed towards supervision, review and editing.

Acknowledgements

This research was financially supported by Statutory Funds of the Department of Molecular and Cellular Biology, no. SUB.D260.20.009 and partially by National Science Centre (Poland) within a framework of SONATA BIS 6 (2016/22/E/NZ5/00671; PI: J. Kulbacka). The research was supported by the Scientific Cancer Cell Biology Group No. 148 (Wroclaw Medical University) and was partially performed in the Screening Laboratory of Biological Activity Test and Collection of Biological Material, Faculty of Pharmacy and the Division of Laboratory Diagnostics, Wroclaw Medical University, supported by the ERDF Project within the Innovation Economy Operational Programme POIG.02.01.00-14-122/09.

References

1 Damsky WE, Rosenbaum LE and Bosenberg M: Decoding melanoma metastasis. Cancers (Basel) *3(1)*: 126-163, 2010. PMID: 24212610. DOI: 10.3390/cancers3010126

2 Kim C, Lee CW, Kovacic L, Shah A, Klasa R and Savage KJ: Long-term survival in patients with metastatic melanoma treated with DTIC or temozolomide. Oncologist *15(7)*: 765-71, 2010. PMID: 20538743. DOI: 10.1634/theoncologist.2009-0237

3 Rastrelli M, Tropea S, Pigozzo J, Bezzon E, Campana LG, Stramare R, Alaibac M and Rossi CR: Melanoma m1: Diagnosis and therapy. In Vivo *28(3)*: 273-285, 2014. PMID: 24815827.

4 Gorayski P, Burmeister B and Foote M: Radiotherapy for cutaneous melanoma: current and future applications. Future Oncol *11(3)*: 525-534, 2015. PMID: 25675130. DOI: 10.2217/fon.14.300

5 Middleton MR, Grob JJ, Aaronson N, Fierlbeck G, Tilgen W, Seiter S, Gore M, Aamdal S, Cebon J, Coates A, Dreno B, Henz M, Schadendorf D, Kapp A, Weiss J, Fraass U, Statkevich P, Muller M and Thatcher N: Randomized phase III study of temozolomide *versus* dacarbazine in the treatment of patients with advanced metastatic malignant melanoma. J Clin Oncol *18(1)*: 158-166, 2000. PMID: 10623706. DOI: 10.1200/JCO.2000.18.1.158

6 Nathan PD and Eisen TG: The biological treatment of renal-cell carcinoma and melanoma. Lancet Oncol *3(2)*: 89-96, 2002. PMID: 11902528. DOI: 10.1016/s1470-2045(02)00650-2

7 Chen TL, Chang JW, Hsieh JJ, Cheng HY and Chiou CC: A sensitive peptide nucleic acid probe assay for detection of BRAF V600 mutations in melanoma. Cancer Genomics Proteomics 13(5): 381-386, 2016. PMID: 27566656.

8 BRAF (v-raf murine sarcoma viral oncogene homolog B1). Available at: http://atlasgeneticsoncology.org/Genes/BRAFID828.html [Last accessed on 07-04-20]

9 Hugdahl E, Kalvenes MB, Puntervoll HE, Ladstein RG and Akslen LA: BRAF-V600E expression in primary nodular melanoma is associated with aggressive tumour features and reduced survival. Br J Cancer *114(7)*: 801-808, 2016. PMID: 26924424. DOI: 10.1038/bjc.2016.44

10 Ascierto PA, Kirkwood JM, Grob JJ, Simeone E, Grimaldi AM, Maio M, Palmieri G, Testori A, Marincola FM and Mozzillo N: The role of BRAF V600 mutation in melanoma. J Transl Med *10*: 85, 2012. PMID: 22554099. DOI: 10.1186/1479-5876-10-85

11 Fujimura T, Hidaka T, Kambayashi Y and Aiba S: BRAF kinase inhibitors for treatment of melanoma: developments from early-stage animal studies to Phase II clinical trials. Expert Opin Investig Drugs *28(2)*: 143-148, 2019. PMID: 30556435. DOI: 10.1080/13543784.2019.1558442

12 Bronte E, Bronte G, Novo G, Bronte F, Bavetta MG, Lo Re G, Brancatelli G, Bazan V, Natoli C, Novo S and Russo A: What links BRAF to the heart function? New insights from the cardiotoxicity of BRAF inhibitors in cancer treatment. Oncotarget *6(34)*: 35589-35601, 2015. PMID: 26431495. DOI: 10.18632/oncotarget.5853

13 Manzano JL, Layos L, Bugés C, de Los Llanos Gil M, Vila L, Martínez-Balibrea E and Martínez-Cardús A: Resistant mechanisms to BRAF inhibitors in melanoma. Ann Transl Med *4(12)*: 237, 2016. PMID: 27429963. DOI: 10.21037/atm.2016.06.07

14 Telang S, Yalcin A, Clem AL, Bucala R, Lane AN, Eaton JW and Chesney J: Ras transformation requires metabolic control by 6-phosphofructo-2-kinase. Oncogene *25*: 7225-7234, 2006. PMID: 16715124. DOI: 10.1038/sj.onc.1209709

15 Kumar SM, Yu H, Edwards R, Chen L, Kazianis S, Brafford P, Acs G, Herlyn M and Xu X: Mutant V600E BRAF increases hypoxia inducible factor-1α expression in melanoma. Cancer Res *67(7)*: 3177-3184, 2007. PMID: 17409425. DOI: 10.1158/0008-5472.CAN-06-3312

16 Obach M, Navarro-Sabaté A, Caro J, Kong X, Duran J, Gómez M, Perales JC, Ventura F, Rosa JL and Bartrons R: 6-Phosphofructo-2-kinase (pfkfb3) gene promoter contains hypoxia-inducible factor-1 binding sites necessary for transactivation in response to hypoxia. J Biol Chem *279(51)*: 53562-53570, 2004. PMID: 15466858. DOI: 10.1074/jbc.M406096200

17 Lu L, Chen Y and Zhu Y: The molecular basis of targeting PFKFB3 as a therapeutic strategy against cancer. Oncotarget *8(37)*: 62793-62802, 2017. PMID: 28977989. DOI: 10.18632/oncotarget.19513

18 Warburg O, Wind F and Negelein E: The metabolism of tumor in the body. J Gen Physiol *8(6)*: 519-30, 1927. PMID: 19872213. DOI: 10.1085/jgp.8.6.519

19 Clem B, Telang S, Clem A, Yalcin A, Meier J, Simmons A, Rasku MA, Arumugam S, Dean WL, Eaton J, Lane A, Trent JO and Chesney J: Small-molecule inhibition of 6-phosphofructo-2-kinase activity suppresses glycolytic flux and tumor growth. Mol Cancer Ther *7(1)*: 110-120, 2008. PMID: 18202014. DOI: 10.1158/1535-7163.MCT-07-0482

20 National Center for Biotechnology Information. PubChem Database. 3PO, >=98% (HPLC), Source=Sigma-Aldrich, "SID 329825800 - PubChem." Available at: https://pubchem.ncbi.nlm.nih.gov/substance/329825800#section=2D-Structure [Last accessed on 30-Dec-2018]

21 Shi L, Pan H, Liu Z, Xie J and Han W: Roles of PFKFB3 in cancer. Signal Transduct Target Ther *2*: 17044, 2017. PMID: 29263928. DOI: 10.1038/sigtrans.2017.44

22 Trojan SE, Piwowar M, Ostrowska B, Laidler P and Kocemba-Pilarczyk KA: Analysis of malignant melanoma cell lines exposed to hypoxia reveals the importance of PFKFB4 overexpression for disease progression. Anticancer Res *38(12)*: 6745-6752, 2018. PMID: 30504385. DOI: 10.21873/anticanres.13044

23 Boyd S, Brookfield JL, Critchlow SE, Cumming IA, Curtis NJ, Debreczeni J, Degorce SL, Donald C, Evans NJ, Groombridge S, Hopcroft P, Jones NP, Kettle JG, Lamont S, Lewis HJ, MacFaull P, McLoughlin SB, Rigoreau LJ, Smith JM, St-Gallay S, Stock JK, Turnbull AP, Wheatley ER, Winter J and Wingfield J: Structure-based design of potent and selective inhibitors of the metabolic kinase PFKFB3. J Med Chem *58(8)*: 3611-3625, 2015. PMID: 25849762. DOI: 10.1021/acs.jmedchem.5b00352

24 Bartrons R, Rodríguez-García A, Simon-Molas H, Castaño E, Manzano A and Navarro-Sabaté À: The potential utility of PFKFB3 as a therapeutic target. Expert Opin Ther Targets *2(8)*: 659-674, 2018. PMID: 29985086. DOI: 10.1080/14728222.2018.1498082

25 Clem BF, O'Neal J, Tapolsky G, Clem AL, Imbert-Fernandez Y, Kerr DA 2nd, Klarer AC, Redman R, Miller DM, Trent JO, Telang S and Chesney J: Targeting 6-phosphofructo-2-kinase (PFKFB3) as a therapeutic strategy against cancer. Mol Cancer Ther *12(8)*: 1461-1470, 2013. PMID: 23674815. DOI: 10.1158/1535-7163.MCT-13-0097

26 Lea MA, Altayyar M and desBordes C: Inhibition of growth of bladder cancer cells by 3-(3-pyridinyl)-1-(4-pyridinyl)-2-propen-1-one in combination with other compounds affecting glucose metabolism. Anticancer Res *35(11)*: 5889-5899, 2015. PMID: 26504012.

27 Wellbrock C and Hurlstone A: BRAF as therapeutic target in melanoma. Biochem Pharmacol *80(5)*: 561-567, 2010. PMID: 20350535. DOI: 10.1016/j.bcp.2010.03.019

28 Bucheit AD and Davies MA: Emerging insights into resistance to BRAF inhibitors in melanoma. Biochem Pharmacol *87(3)*: 381-389, 2014. PMID: 24291778. DOI: 10.1016/j.bcp.2013.11.013

29 Hanwell MD, Curtis DE, Lonie DC, Vandermeersch T, Zurek E and Hutchison GR: Avogadro: an advanced semantic chemical editor, visualization, and analysis platform. J Cheminform *4(1)*: 17, 2012. PMID: 22889332. DOI: 10.1186/1758-2946-4-17

30 Halgren TA: Merck molecular force field. III. Molecular geometries and vibrational frequencies for MMFF94. J Comput Chem *17(5-6)*: 533-586, 1996. DOI: 10.1002/(SICI)1096-987X(199604)17:5/6<553::AID-JCC3>3.0.CO;2-T

31 Frisch MJ, Trucks GW and Schlegel HB: Gaussian 16 Revision B. 01 Release Notes, 2018. Available at: https://gaussian.com/relnotes_b01/

32 Goerigk L and Grimme S: Efficient and accurate double-hybrid-meta-GGA density functionals-evaluation with the extended GMTKN30 database for general main group thermochemistry, kinetics, and noncovalent interactions. J Chem Theory Comput *7(2)*: 291-309, 2011. DOI: 10.1021/ct100466k

33 Weigend F and Ahlrichs R: Balanced basis sets of split valence, triple zeta valence and quadruple zeta valence quality for H to Rn: Design and assessment of accuracy. Phys Chem Chem Phys *7(18)*: 3297-3305, 2005. PMID: 16240044. DOI: 10.1039/b508541a

34 Carlson HA, Smith RD, Damm-Ganamet KL, Stuckey JA, Ahmed A, Convery MA, Somers DO, Kranz M, Elkins PA, Cui G, Peishoff CE, Lambert MH and Dunbar JB Jr: CSAR 2014: A benchmark exercise using unpublished data from pharma. J Chem Inf Model *56(6)*: 1063-1077, 2016. PMID: 27149958. DOI: 10.1021/acs.jcim.5b00523

35 Trott O and Olson AJ: Software news and update AutoDock Vina: Improving the speed and accuracy of docking with a new scoring function, efficient optimization, and multithreading. J Comput Chem *31(2)*: 455-461, 2010. PMID: 19499576. DOI: 10.1002/jcc.21334

36 Quiroga R and Villarreal MA: Vinardo: A scoring function based on autodock vina improves scoring, docking, and virtual screening. PLoS One *11(5)*, 2016. PMID: 27171006. DOI: 10.1371/journal.pone.0155183

37 Wang R, Lu Y, Fang X and Wang S: An extensive test of 14 scoring functions using the PDBbind refined set of 800 protein–ligand complexes. J Chem Inf Comput Sci *44(6)*: 2114-2125, 2004. PMID: 15554682. DOI: 10.1021/ci049733j

38 Humphrey W, Dalke A and Schulten K: VMD: Visual molecular dynamics. J Mol Graph *14(1)*: 33-38, 1996. PMID: 8744570. DOI: 10.1016/0263-7855(96)00018-5

39 Michel O, Kulbacka J, Saczko J, Mączyńska J, Błasiak P, Rossowska J and Rzechonek A: Electroporation with cisplatin against metastatic pancreatic cancer. *In vitro* study on human primary cell culture. Biomed Res Int *2018*: 7364539, 2018. PMID: 29750170. DOI: 10.1155/2018/7364539

40 Crowley LC, Marfell BJ, Scott AP and Waterhouse NJ: Quantitation of apoptosis and necrosis by annexin V binding, propidium iodide uptake, and flow cytometry. Cold Spring Harb Protoc, 2016. PMID: 27803250. DOI: 10.1101/pdb.prot087288

41 Franken NA, Rodermond HM, Stap J, Haveman J and van Bree C: Clonogenic assay of cells *in vitro*. Nat Protoc *1*: 2315-2319, 2006. PMID: 17406473. DOI: 10.1038/nprot.2006.339

42 Wlodkowic D, Skommer J and Darzynkiewicz Z: Flow cytometry-based apoptosis detection. Methods Mol Biol *559*: 19-32, 2009. PMID: 19609746. DOI: 10.1007/978-1-60327-017-5_2

43 Laikova KV, Oberemok VV, Krasnodubets AM, Gal'chinsky NV, Useinov RZ, Novikov IA, Temirova ZZ, Gorlov MV, Shved NA, Kumeiko VV, Makalish TP, Bessalova EY, Fomochkina II, Esin AS, Volkov ME and Kubyshkin AV: Advances in the understanding of skin cancer: Ultraviolet radiation, mutations, and antisense oligonucleotides as anticancer drugs. Molecules *24(8)*, 2019. PMID: 30999681. DOI: 10.3390/molecules24081516

44 Ultraviolet radiation (UV). Skin cancers. Available at: https://www.who.int/uv/faq/skincancer/en/index1.html?fbclid=IwAR1X91w6Fpj7ncEMMXBcuN1yytdkMjzGDDKEW4S0ShewHw21u0ro6zftjF4 [Last accessed on 07-04-20]

45 Gençler B and Gönül M: Cutaneous side effects of BRAF inhibitors in advanced melanoma: review of the literature. Dermatol Res Pract *2016*: 5361569, 2016. PMID: 27042173. DOI: 10.1155/2016/5361569

46 Ryabaya O, Prokofieva A, Akasov R, Khochenkov D, Emelyanova M, Burov S, Markvicheva E, Inshakov A and Stepanova E: Metformin increases antitumor activity of MEK inhibitor binimetinib in 2D and 3D models of human metastatic melanoma cells. Biomed Pharmacother *109*: 2548-2560, 2018. PMID: 30551515. DOI: 10.1016/j.biopha.2018.11.109

47 Xintaropoulou C, Ward C, Wise A, Marston H, Turnbull A and Langdon SP: A comparative analysis of inhibitors of the glycolysis pathway in breast and ovarian cancer cell line models.

Oncotarget *6(28)*: 25677-25695, 2015. PMID: 26259240. DOI: 10.18632/oncotarget.4499

48 Chowdhury N, Vhora I, Patel K, Doddapaneni R, Mondal A and Singh M: Liposomes co-loaded with 6-phosphofructo-2-kinase/fructose-2, 6-biphosphatase 3 (PFKFB3) shRNA plasmid and docetaxel for the treatment of non-small cell lung cancer. Pharm Res *34(11)*: 2371-2384, 2017. PMID: 28875330. DOI: 10.1007/s11095-017-2244-x

49 Feng Y and Wu L: mTOR up-regulation of PFKFB3 is essential for acute myeloid leukemia cell survival. Biochem Biophys Res Commun *483(2)*: 897-903, 2017. PMID: 28082200. DOI: 10.1016/j.bbrc.2017.01.031

50 Wang L, Wu J, Lu J, Ma R, Sun D and Tang J: Regulation of the cell cycle and PI3K/Akt/mTOR signaling pathway by tanshinone I in human breast cancer cell lines. Mol Med Rep *11(2)*: 931-939, 2015. PMID: 25355053. DOI: 10.3892/mmr.2014.2819

51 Klarer AC, O'Neal J, Imbert-Fernandez Y, Clem A, Ellis SR, Clark J, Clem B, Chesney J and Telang S: Inhibition of 6-phosphofructo-2-kinase (PFKFB3) induces autophagy as a survival mechanism. Cancer Metab *2(1)*: 2, 2014. PMID: 24451478. DOI: 10.1186/2049-3002-2-2

52 Wang C, Qu J, Yan S, Gao Q, Hao S and Zhou D: PFK15, a PFKFB3 antagonist, inhibits autophagy and proliferation in rhabdomyosarcoma cells. Int J Mol Med *42(1)*: 359-367, 2018. PMID: 29620138. DOI: 10.3892/ijmm.2018.3599

53 Yan S, Wei X, Xu S, Sun H, Wang W, Liu L, Jiang X, Zhang Y and Che Y: 6-Phosphofructo-2-kinase/fructose-2,6-bisphosphatase isoform 3 spatially mediates autophagy through the AMPK signaling pathway. Oncotarget *8(46)*: 80909-80922, 2017. PMID: 29113354. DOI: 10.18632/oncotarget.20757

54 Hamanaka RB and Mutlu GM: PFKFB3, a direct target of p63, is required for proliferation and inhibits differentiation in epidermal keratinocytes. J Invest Dermatol *137(6)*: 1267-1276, 2017. PMID: 28108301. DOI: 10.1016/j.jid.2016.12.020

55 Lu Q, Yan S, Sun H, Wang W, Li Y, Yang X, Jiang X, Che Y and Xi Z: Akt inhibition attenuates rasfonin-induced autophagy and apoptosis through the glycolytic pathway in renal cancer cells. Cell Death Dis *6(12)*: e2005, 2015. PMID: 26633711. DOI: 10.1038/cddis.2015.344

56 Zhu W, Ye L, Zhang J, Yu P, Wang H, Ye Z and Tian J: PFK15, a small molecule inhibitor of PFKFB3, induces cell cycle arrest, apoptosis and inhibits invasion in gastric cancer. PLoS One *11(9)*: e0163768, 2016. PMID: 27669567. DOI: 10.1371/journal.pone.0163768

57 Yalcin A, Clem BF, Imbert-Fernandez Y, Ozcan SC, Peker S, O'Neal J, Klarer AC, Clem AL, Telang S and Chesney J: 6-Phosphofructo-2-kinase (PFKFB3) promotes cell cycle progression and suppresses apoptosis *via* Cdk1-mediated phosphorylation of p27. Cell Death Dis *5(7)*: e1337-e1337, 2014. PMID: 25032860. DOI: 10.1038/cddis.2014.292

58 Xintaropoulou C, Ward C, Wise A, Queckborner S, Turnbull A, Michie CO, Williams ARW, Rye T, Gourley C and Langdon SP: Expression of glycolytic enzymes in ovarian cancers and evaluation of the glycolytic pathway as a strategy for ovarian cancer treatment. BMC Cancer *18(1)*: 636, 2018. PMID: 29866066. DOI: 10.1186/s12885-018-4521-4

59 O'Neal J, Tapolsky G, Clem B, Telang S and Chesney J: Identification of a PFKFB3 inhibitor suitable for phase I trial testing that synergizes with the B-Raf inhibitor vemurafenib. Cancer Res *74(19) Supplement*: 962-962, 2014. DOI: 10.1158/1538-7445.AM2014-962

60 Conradi LC, Brajic A, Cantelmo AR, Bouché A, Kalucka J, Pircher A, Brüning U, Teuwen LA, Vinckier S, Ghesquière B, Dewerchin M and Carmeliet P: Tumor vessel disintegration by maximum tolerable PFKFB3 blockade. Angiogenesis *20(4)*: 599-613, 2017. PMID: 28875379. DOI: 10.1007/s10456-017-9573-6

61 Mishra DK, Shandilya R and Mishra PK: Lipid based nanocarriers: a translational perspective. Nanomedicine *14(7)*: 2023-2050, 2018. PMID: 29944981. DOI: 10.1016/j.nano.2018.05.021

62 Wakaskar RR: Promising effects of nanomedicine in cancer drug delivery. J Drug Target *26(4)*: 319-324, 2018. PMID: 28875739. DOI: 10.1080/1061186X.2017.1377207

63 Shi J, Ma Y, Zhu J, Chen Y, Sun Y, Yao Y, Yang Z and Xie J: A review on electroporation-based intracellular delivery. Molecules *23(11)*, 2018. PMID: 30469344. DOI: 10.3390/molecules23113044

64 Qin J, Wang TY and Willmann JK: Sonoporation: Applications for cancer therapy. Adv Exp Med Biol *880*: 263-291, 2016. PMID: 26486343. DOI: 10.1007/978-3-319-22536-4_15

Received March 10, 2020
Revised March 30, 2020
Accepted April 8, 2020